Star Formation News Letter #306 No. 45-54

No. 45 The Impact of Feedback in Massive Star Formation. II. Lower Star Formation Efficiency, K.I. Tanaka et al.
No. 46 A Kinematical Detection of Two Embedded Jupiter Mass Planets in HD 163296, R. Teague et al.
No. 47 The Evolution of Protoplanetary Disks: Probing the Inner Disk of Very Low Accretors, T. Thanathibodee et al.
No. 48 Warm CO gas generated by possible turbulent shocks in a low-mass star-forming dense, K. Tokuda et al.
No. 49 The Millimeter Continuum Size-Frequency Relationship in the UZ Tau E Disk, A. Tripathi et al.
No. 50 Magnetic Seismology of Interstellar Gas Clouds: Unveiling a Hidden Dimension, A. Tritsis et al.
No. 51 Disruption of circumstellar discs by large-scale stellar magnetic fields, Asif ud-Doula et al.
No. 52 V1094 Sco: a rare giant multi-ringed disk around a T Tauri star,
S.E. van Terwisga et al.
No. 53 VLTI/MIDI atlas of disks around low- and intermediate-mass young stellar object, VLTI/MIDI atlas of disks around low- and intermediate-mass young stellar object
No. 54 Giant planets around FGK stars form probably through core accretion, Wei Wang et al.

花輪 知幸

No. 45 The Impact of Feedback in Massive Star Formation. II. Lower Star Formation Efficiency, K.I. Tanaka et al. ApJ,

Tanaka+17b を low metallicity に拡張

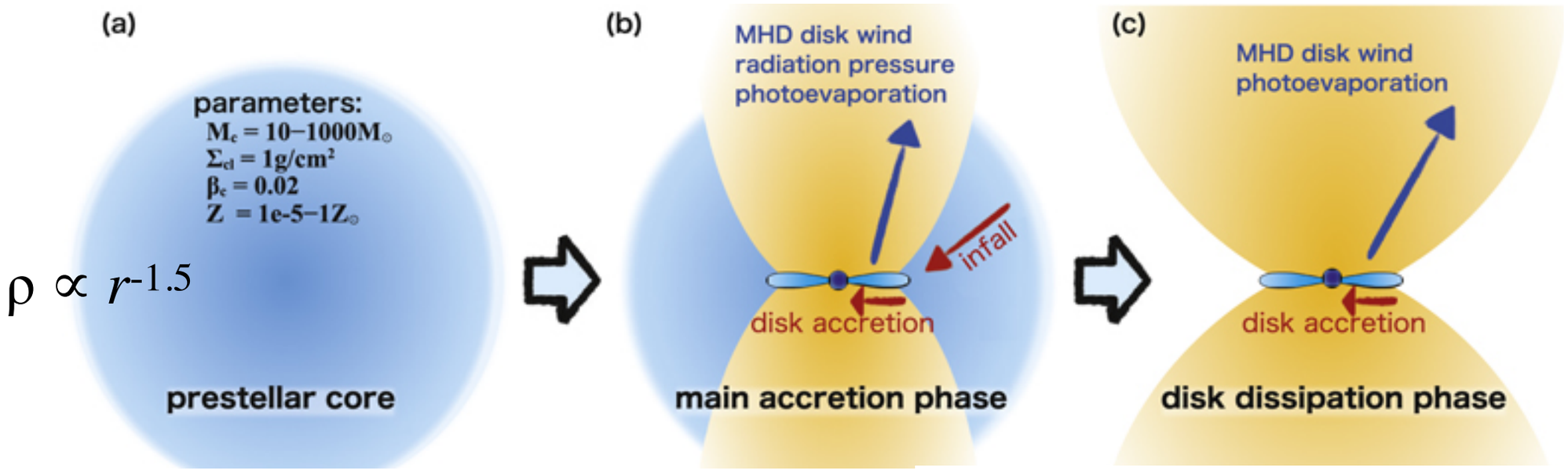

$\rho \propto r^{-1.5}$

$$\dot{M}_{*\mathrm{d}}(t) = 9.2\times10^{-4}\left(\frac{M_{*\mathrm{d}}}{M_c}\right)^{0.5} \times\left(\frac{M_c}{60\,M_\odot}\right)^{3/4}\left(\frac{\Sigma_{\mathrm{cl}}}{1\,\mathrm{g\,cm^{-2}}}\right)^{3/4} M_\odot\,\mathrm{yr}^{-1},$$

$$r_d(t) = 156\left(\frac{\beta_c}{0.02}\right)\left(\frac{M_{*\mathrm{d}}}{m_{*\mathrm{d}}}\right)\left(\frac{M_{*\mathrm{d}}}{M_c}\right)^{2/3} \times\left(\frac{M_c}{60\,M_\odot}\right)^{1/2}\left(\frac{\Sigma_{\mathrm{cl}}}{1\,\mathrm{g\,cm^{-2}}}\right)^{1/2}\mathrm{AU}$$

$$\dot{m}_* = \mu_{\mathrm{esc}}\dot{M}_{*\mathrm{d}} - \dot{m}_{\mathrm{d}} - \dot{m}_{\mathrm{dw}} - \dot{M}_{\mathrm{pe}}, \qquad \dot{m}_{\mathrm{d}} = \dot{m}_*/3 \qquad m_{\mathrm{d}} = m_*/3$$

Feed back: 円盤風, 光蒸発

low metallicity では Opacity が小さいために光蒸発が有効に働く

極端に金属量が低いと重い星は出来にくい。

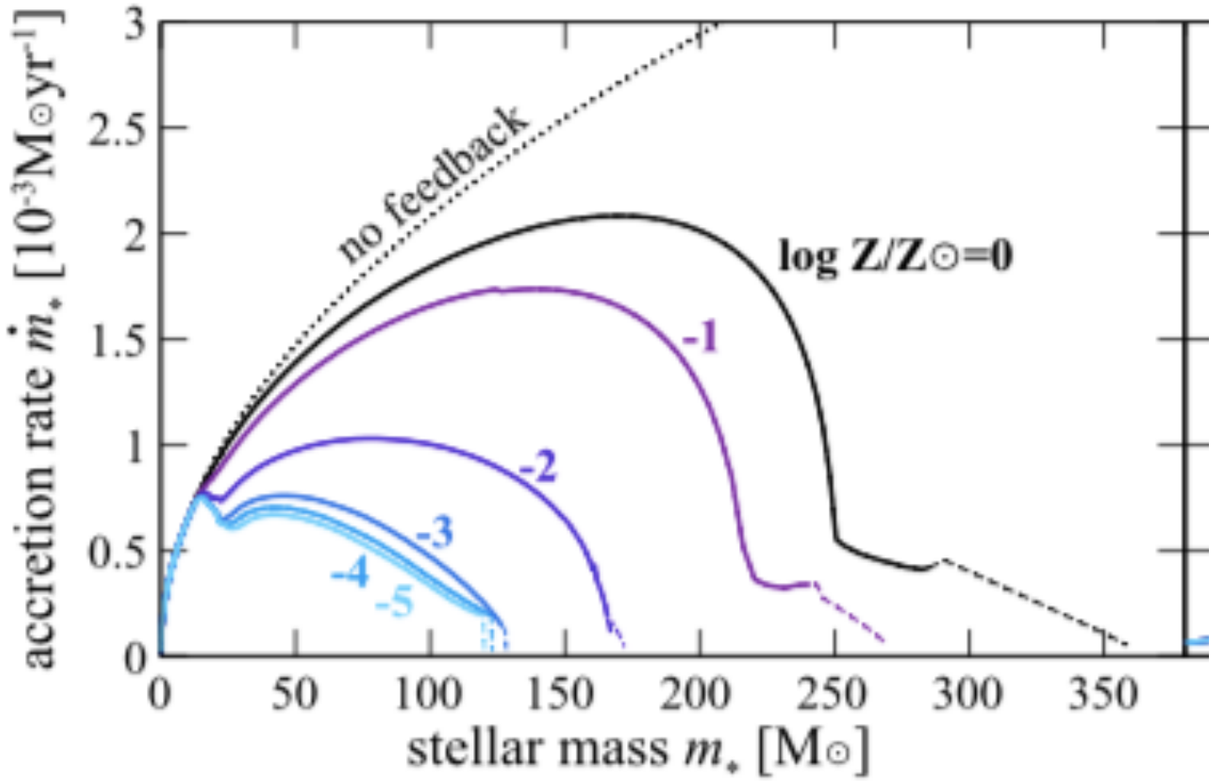

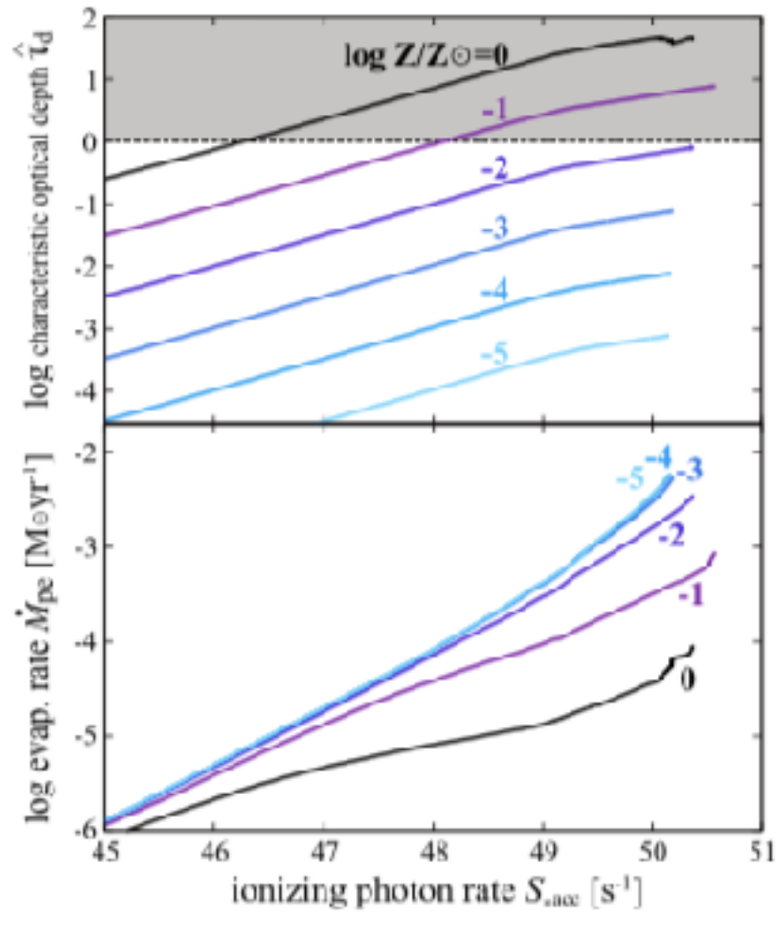

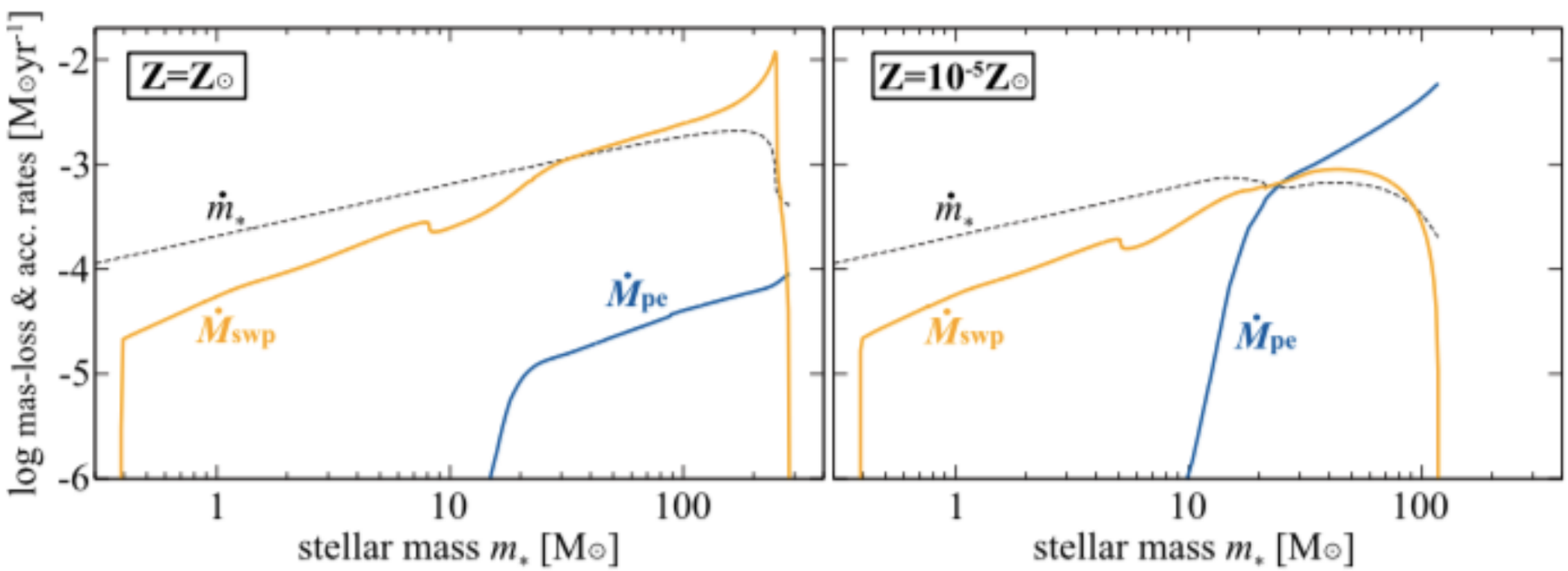

No. 46 A Kinematical Detection of Two Embedded Jupiter Mass Planets in HD 163296, Richard Teague et al. ApJL, 860, L12

$d = 101.5$ pc

two Jupiter-mass planets at 83 and 137 au

No. 38 Kinematic Evidence for an Embedded Protoplanet in a Circumstellar Disk, C. Pinte et al., ApJL, 860, L13

a two-Jupiter-mass planet orbiting at a radius ≈260 au

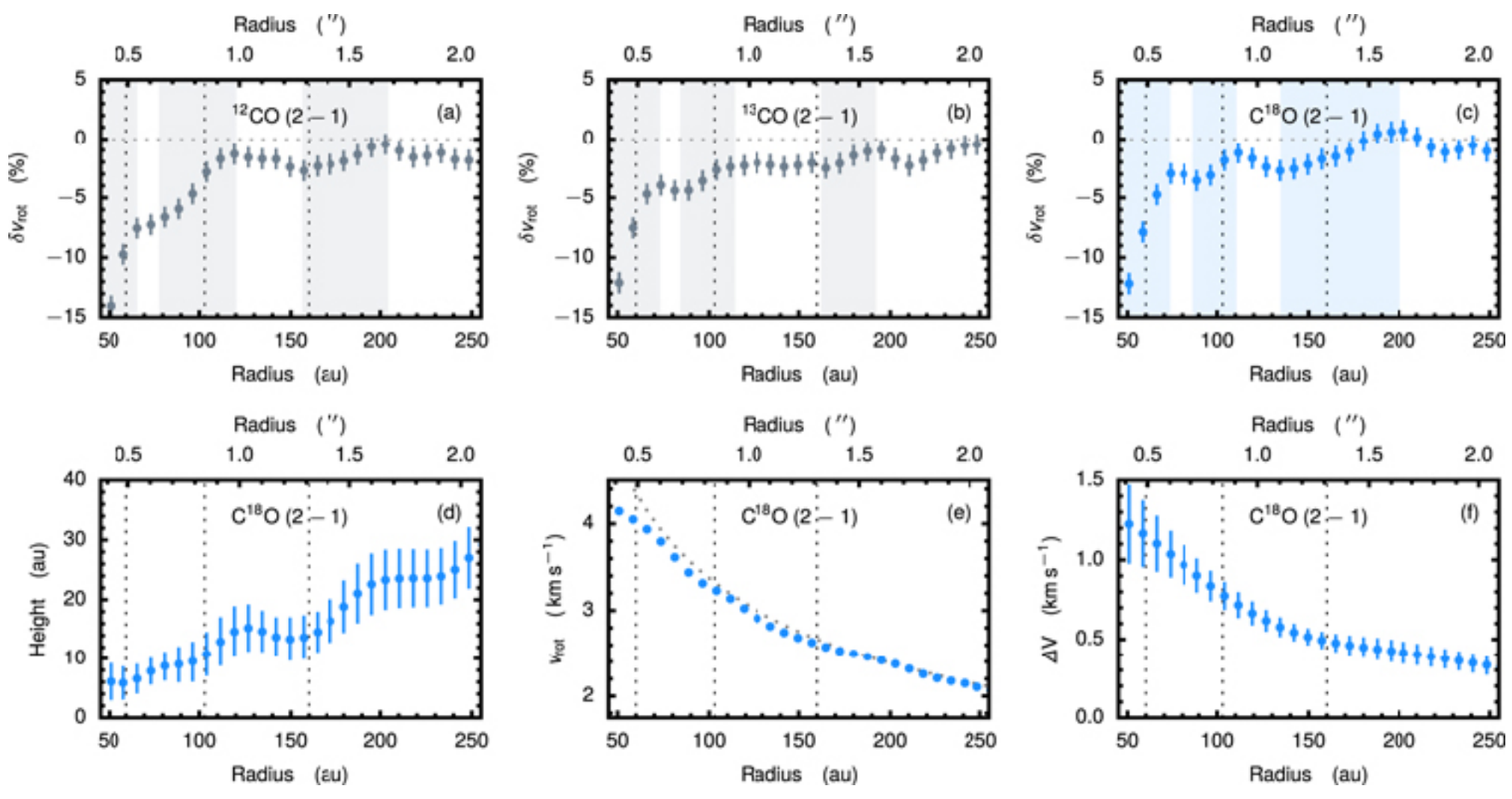

← Kepler 回転からのずれ

cf.
Isella+16, 18
r = 56, 105, 160 au
(continuum)

解析の方針:　円盤は軸対称　　$2.3\ M_\odot,\ i = 47°7,$

$$\frac{v_{\rm rot}^2}{r} = \frac{GM_* r}{(r^2+z^2)^{3/2}} + \frac{1}{\rho_{\rm gas}}\frac{\partial P}{\partial r},$$

円盤の厚み z による減速を考慮

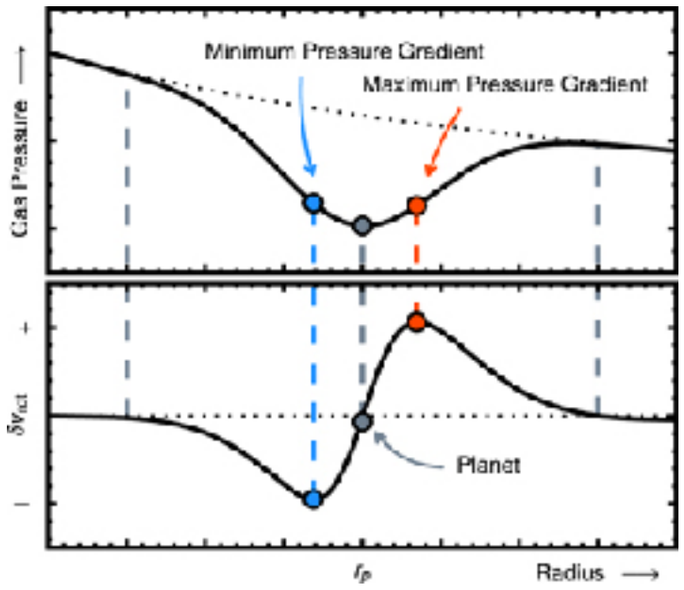

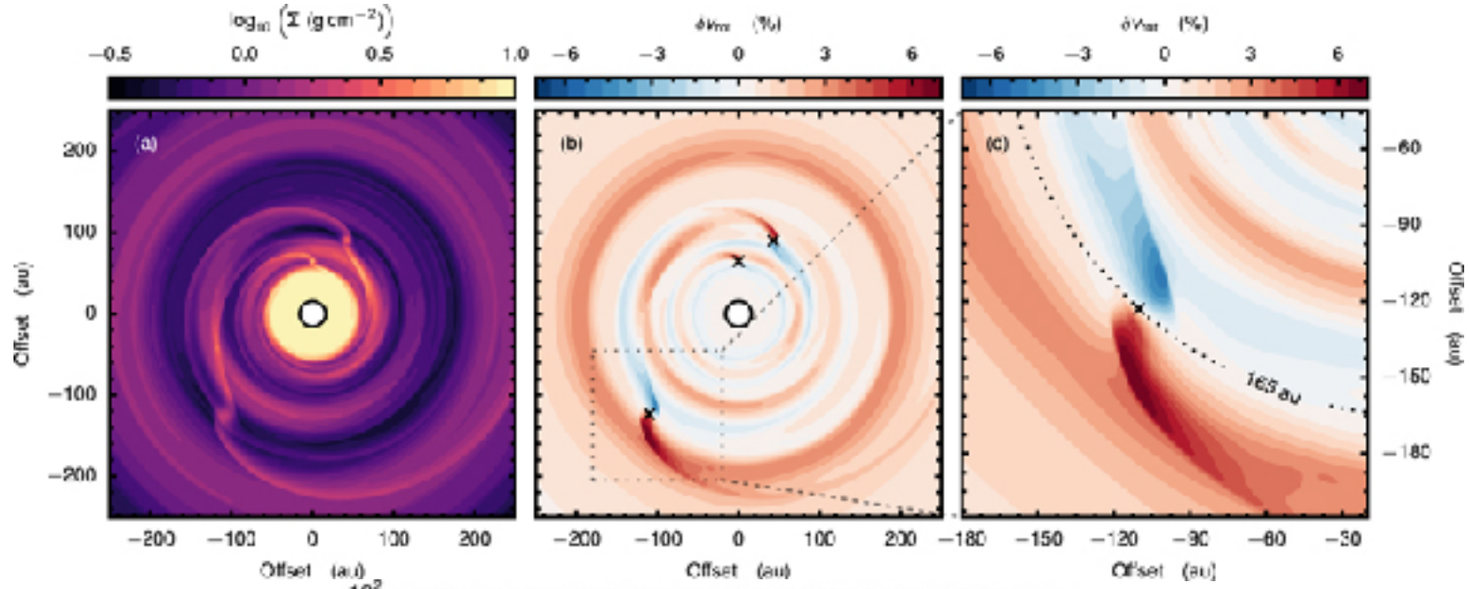

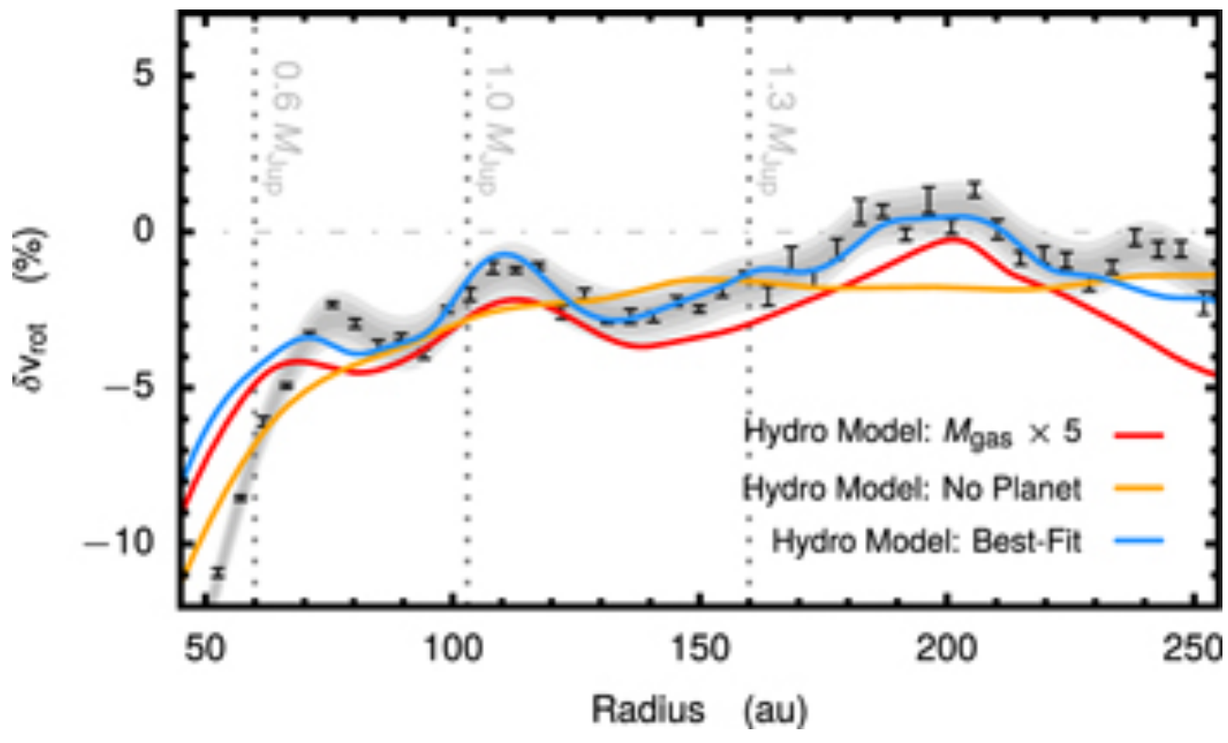

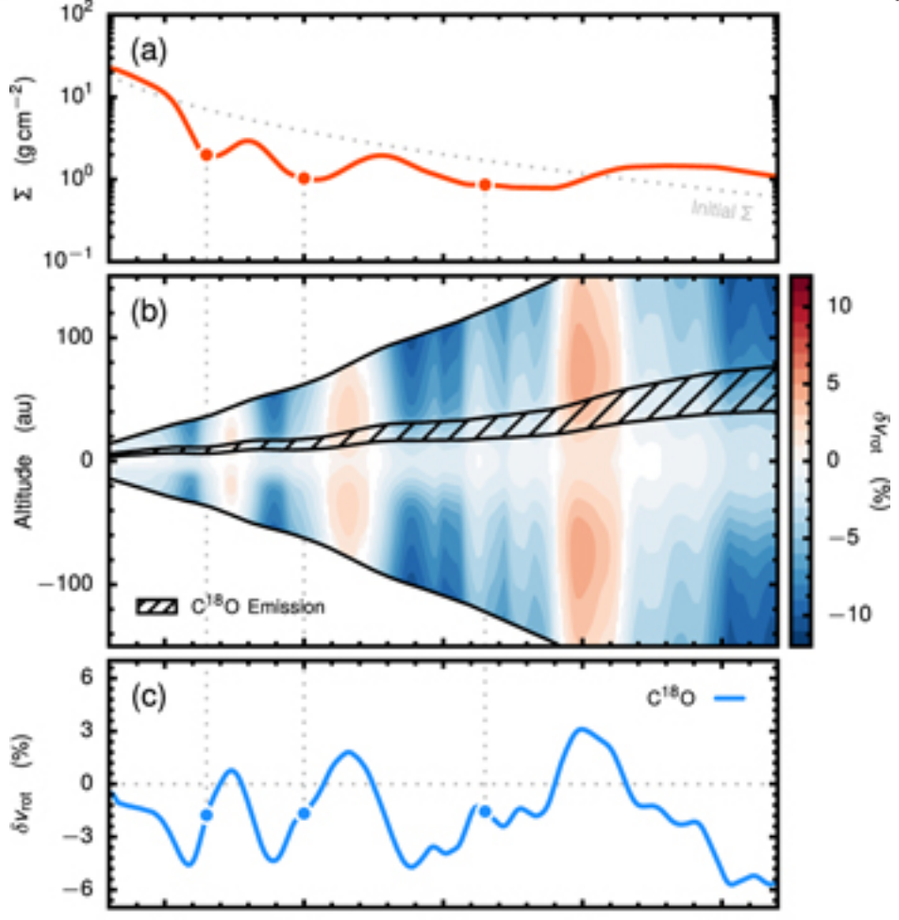

2D

$\alpha = 10^{-3}$

$C^{18}O$

No. 47 The Evolution of Protoplanetary Disks: Probing the Inner Disk of Very Low Accretors, Thanathibodee et al. ApJ, 861, 73

CVSO = CIDA Variability Survey of Orion

降着率が高い順

CVSO 114NE
CVSO 1335
CVSO 114SW

低い降着率の中にも違いがある

diversity

Hα

He I λ10830

H² λ1600

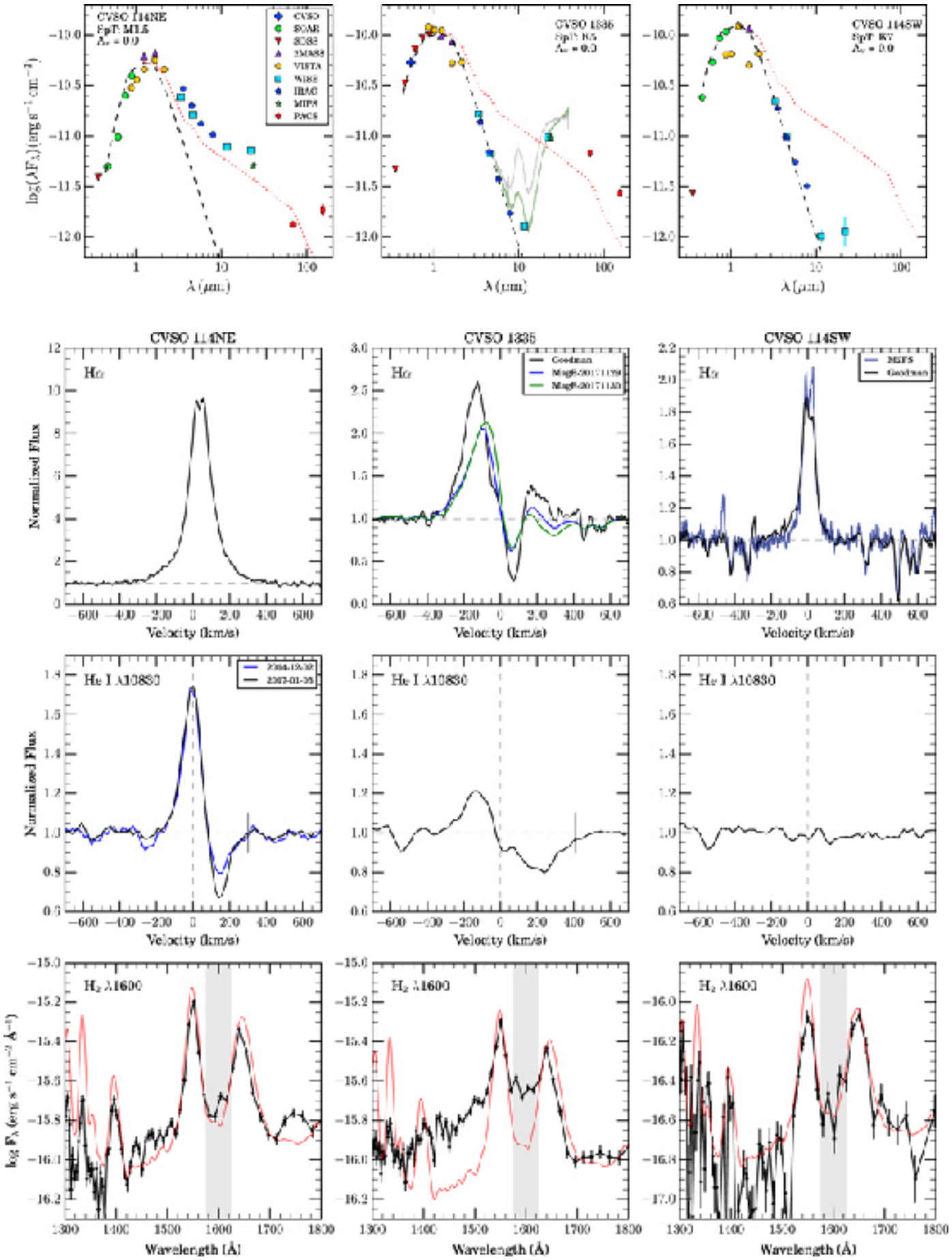

No. 48 Warm CO gas generated by possible turbulent shocks in a low-mass star-forming dense, K. Tokuda et al. ApJ,

MC27/L1521F (MMS-1, 2, 3) Tokuda+14, 16, 17 の follow up

ALMA cycle 3 ^{12}CO (J=3-2), ^{13}CO(J=2-1), C^{18}O (J=2-1)

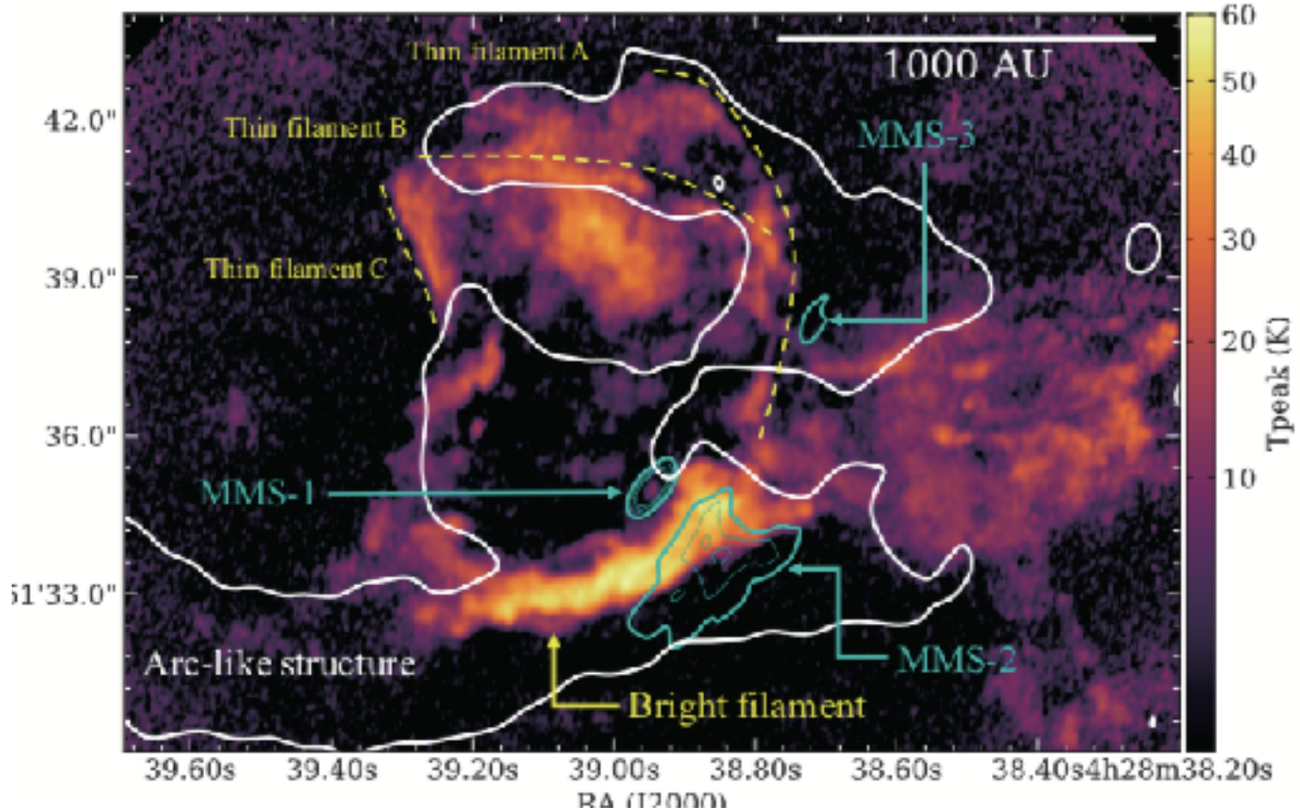

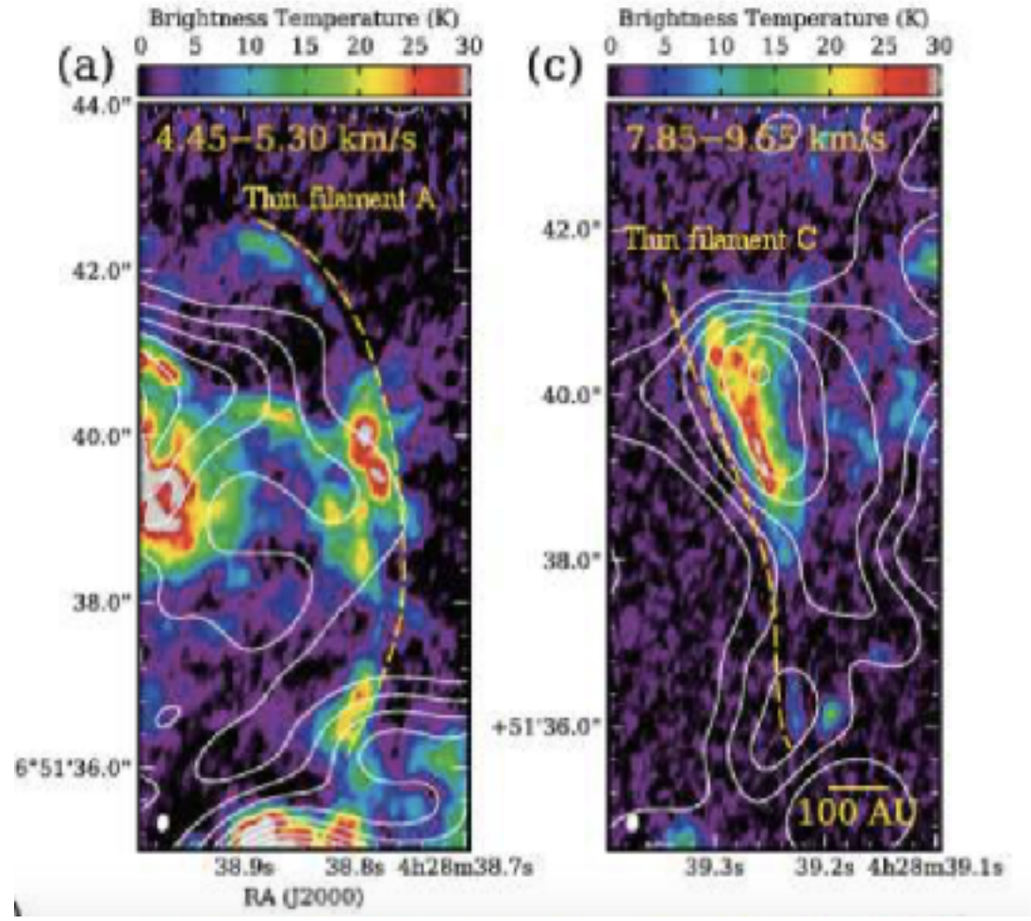

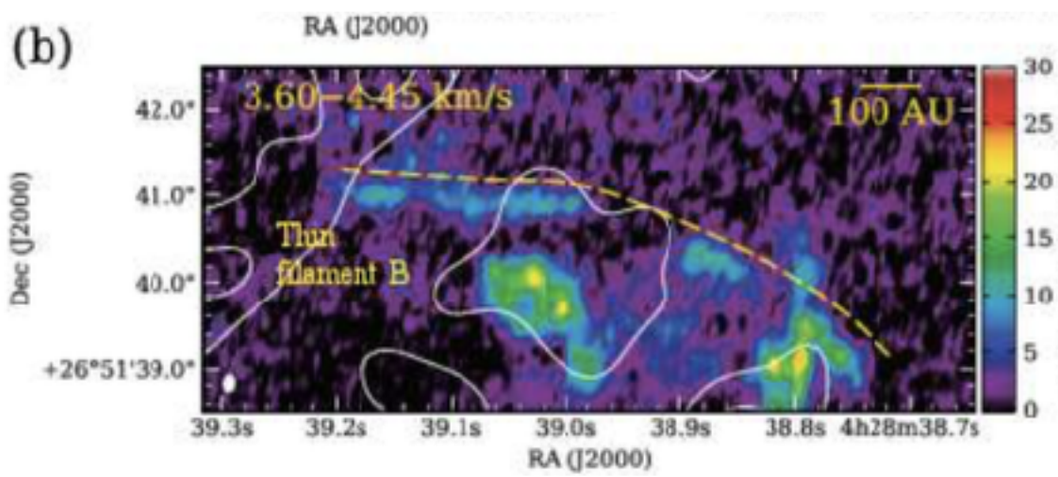

1. warm (15-60 K) filaments (1-2×10^3 au) and clumps (～30 au).
2. 高密度コアとアークは ややred shifted.
3. 高温成分は衝突起源か?

No. 49 The Millimeter Continuum Size-Frequency Relationship in the UZ Tau E Disk, A. Tripathi et al., ApJ, 861, 64

VLA

SMA

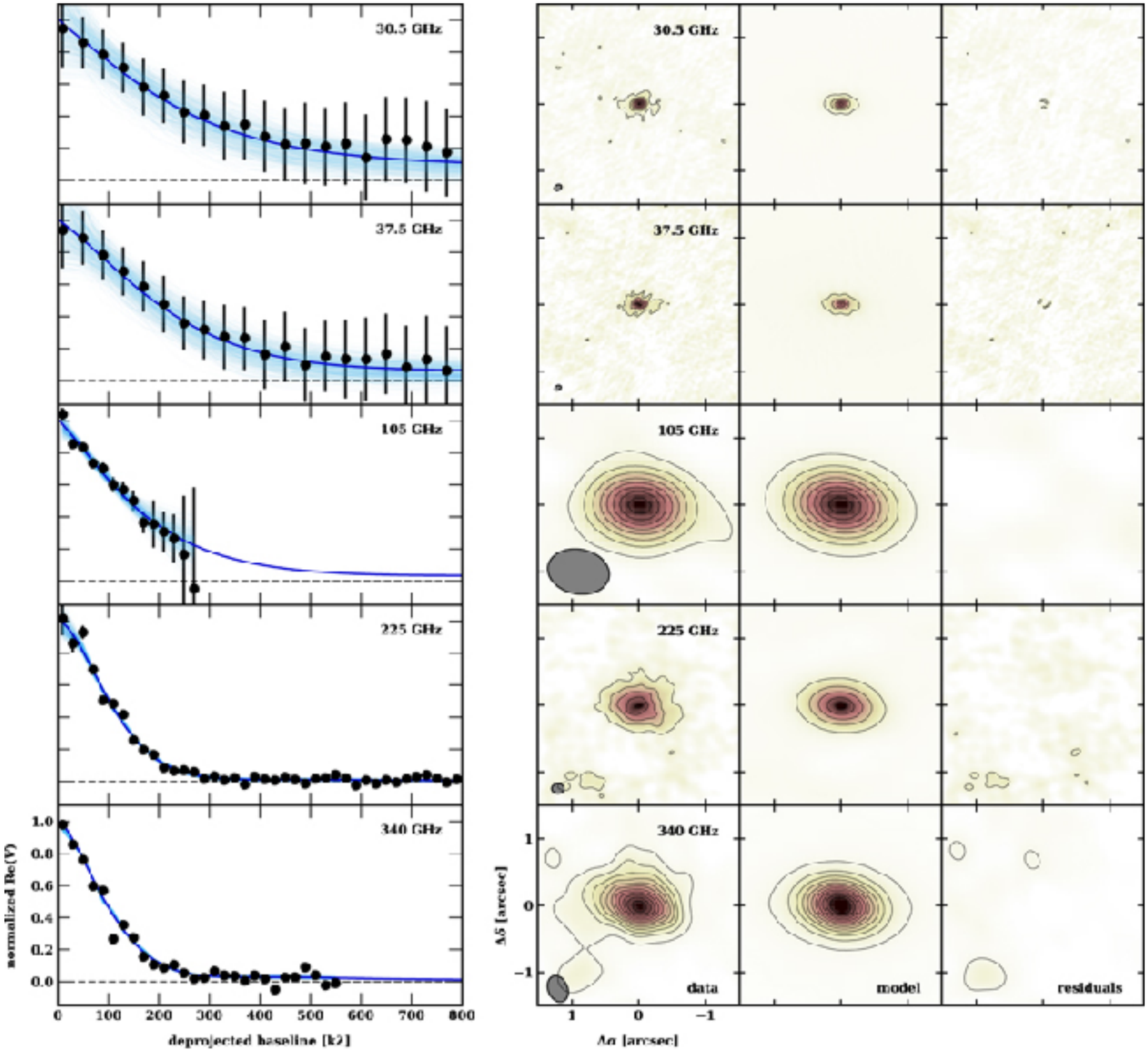

成長と移動を考慮したモデルとの比較

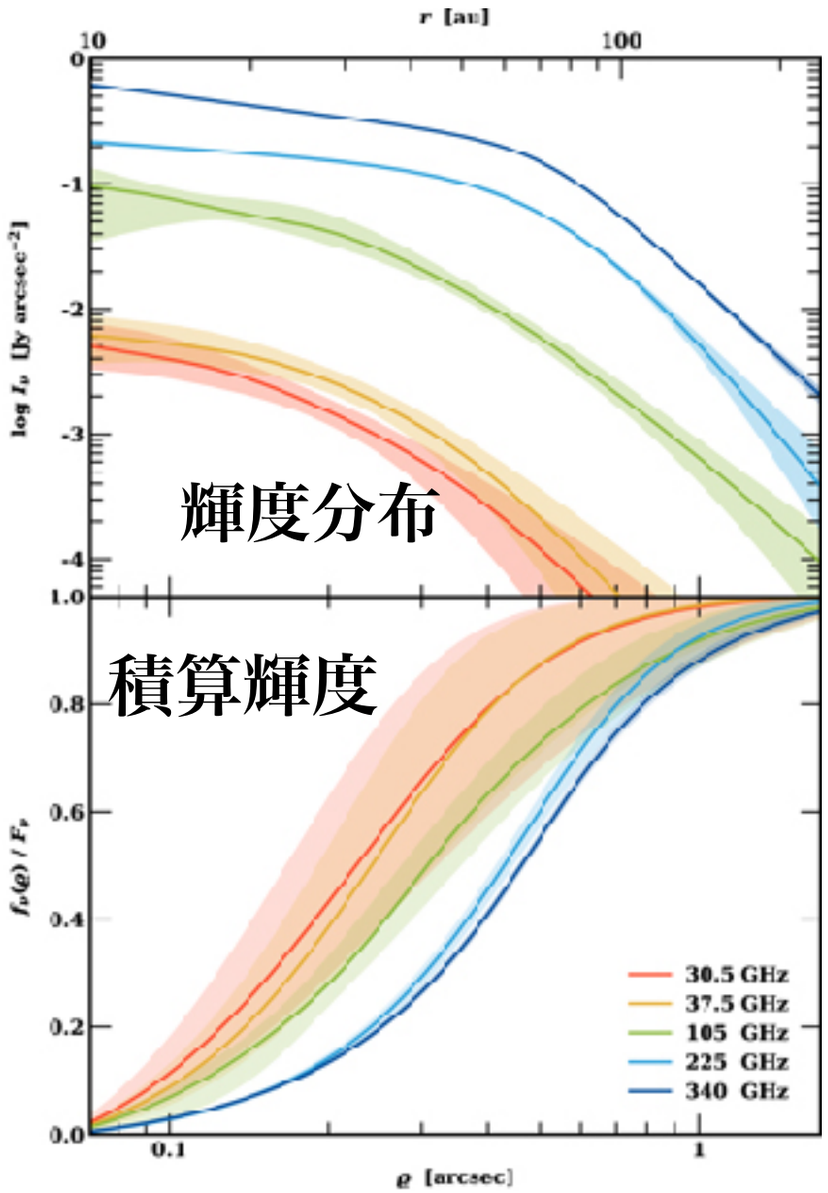

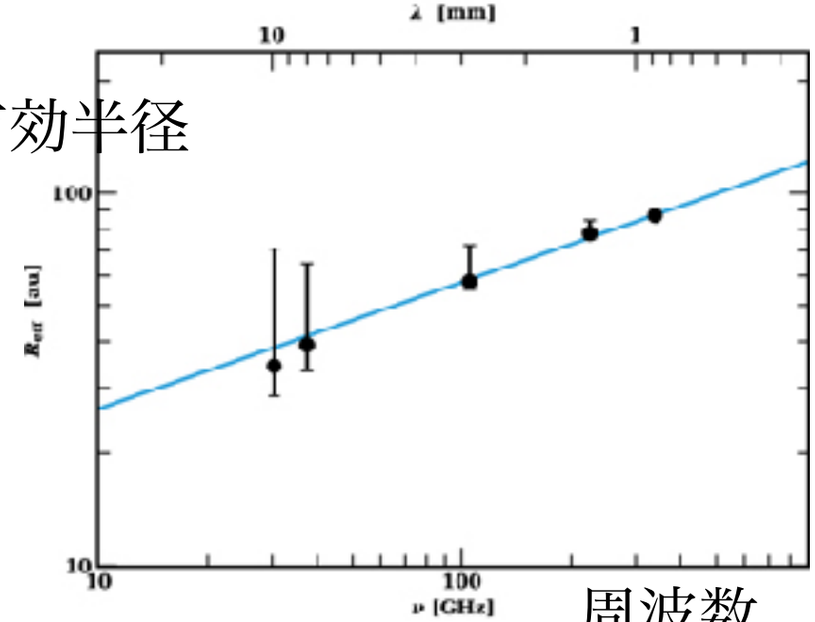

有効半径

周波数

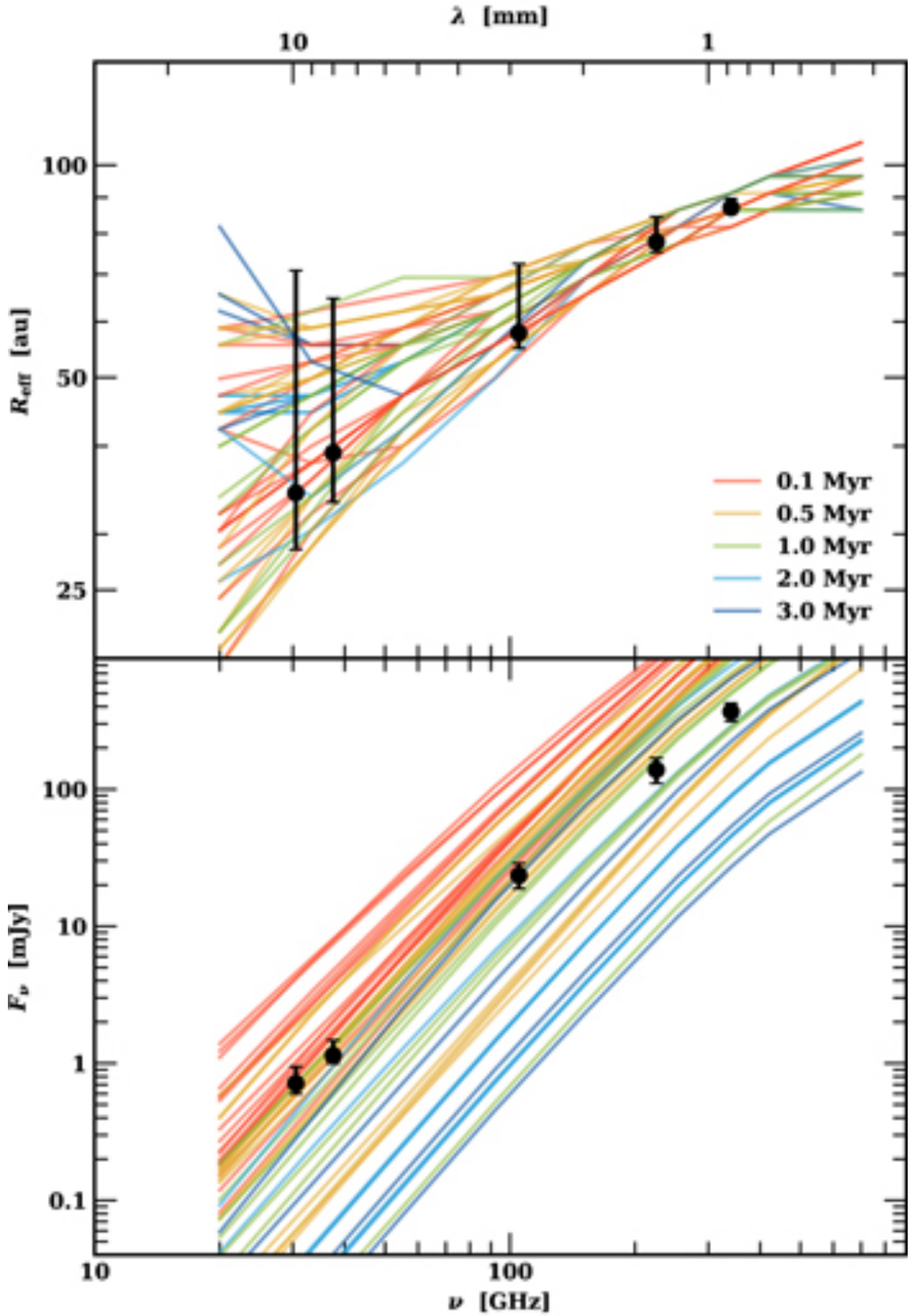

異様に若いと思わないと合わない

No. 50 Magnetic seismology of interstellar gas clouds: Unveiling a hidden dimension, A. Tritsis & K. Tassis, Science, 360, 635

Musca cloud はフィラメントじゃない、edge-on シートだ!

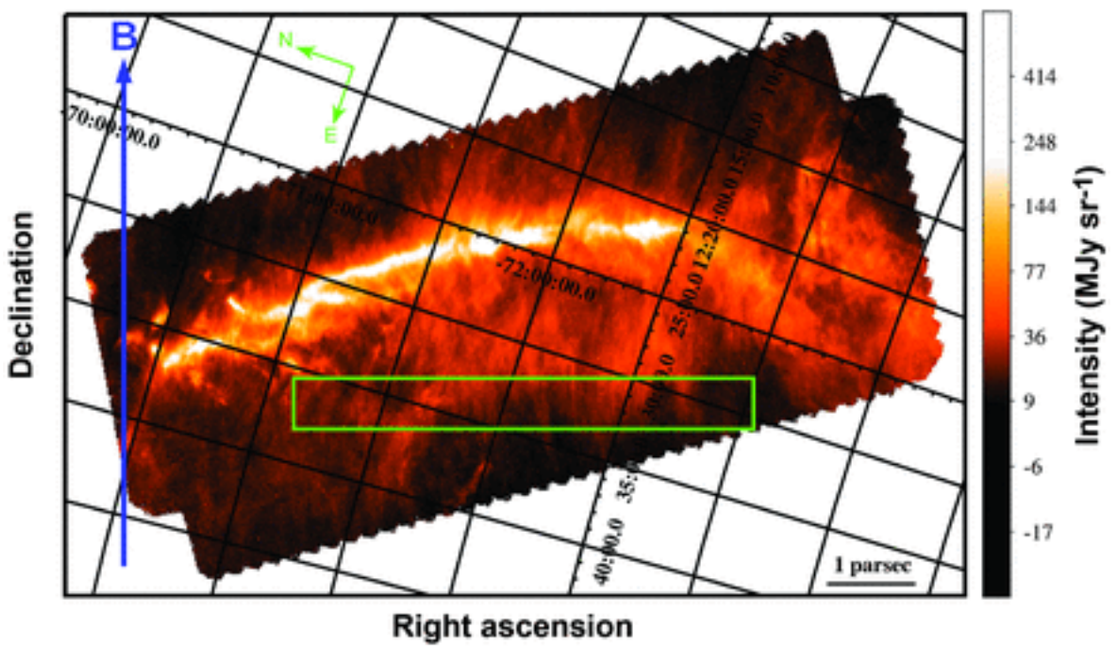

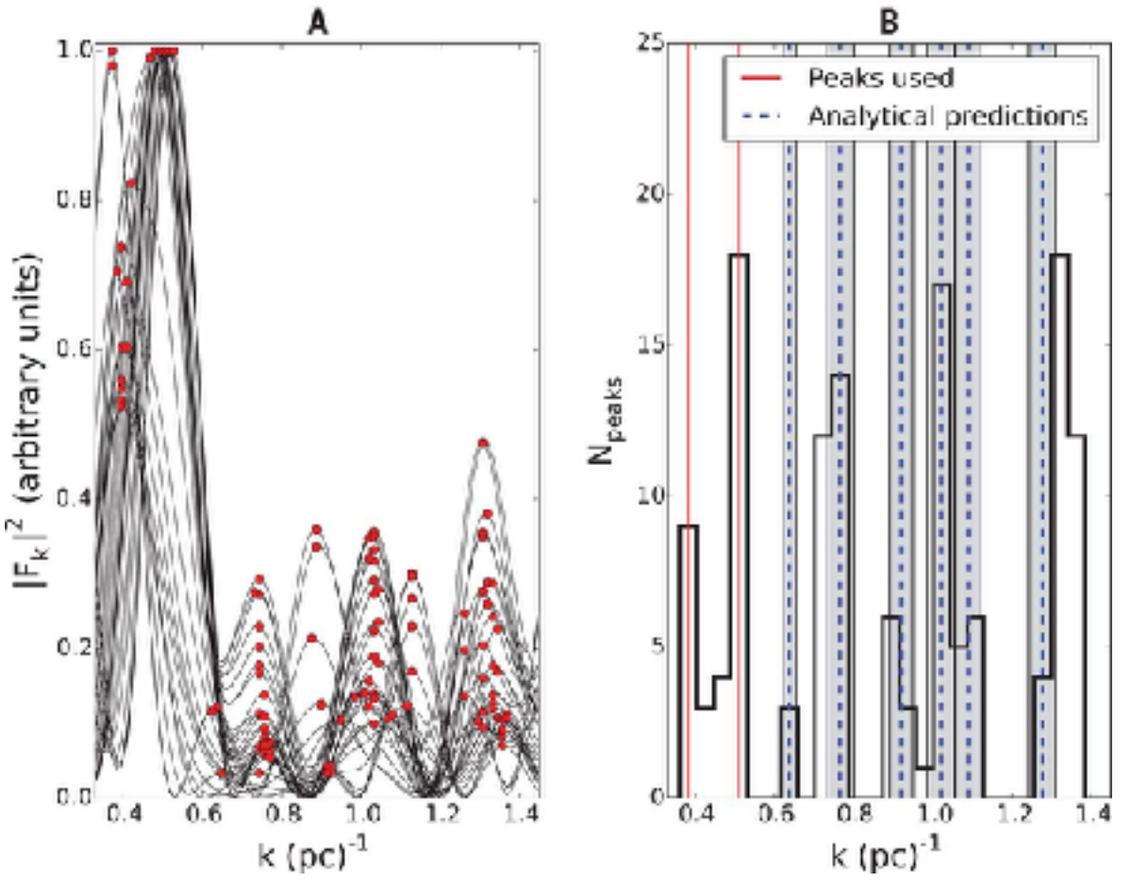

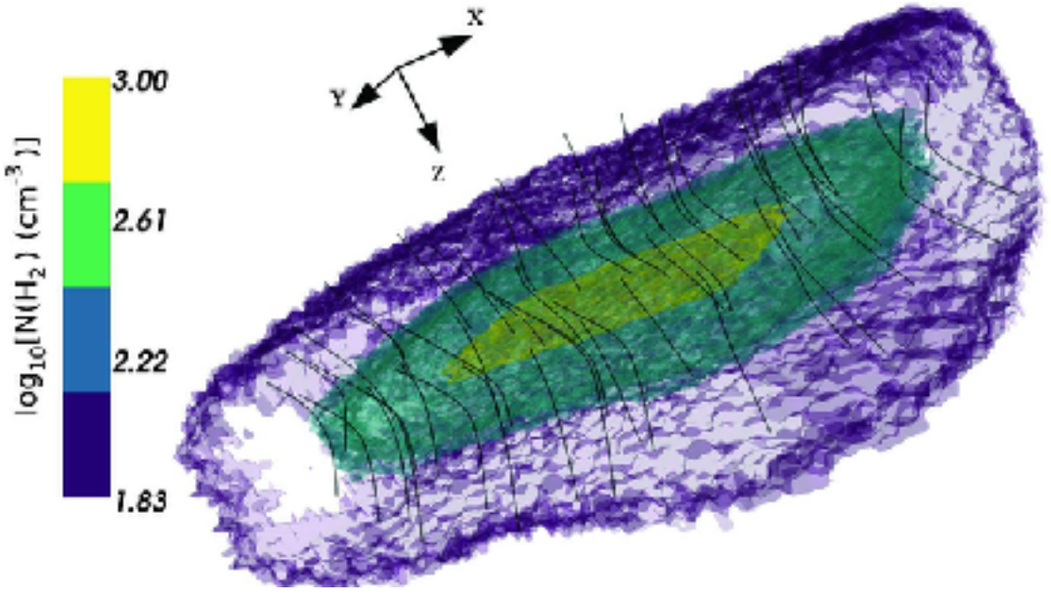

シートの厚みに対応した揺らぎのピークが見られる

$$k_{nm} = \sqrt{\left(\frac{\pi n}{L_x}\right)^2 + \left(\frac{\pi m}{L_y}\right)^2}$$

No. 51 Disruption of circumstellar discs by large-scale stellar magnetic fields, ud-Doula et al., MNRaS, 478, pp. 3049-3055

Be 星には強い磁場がない。

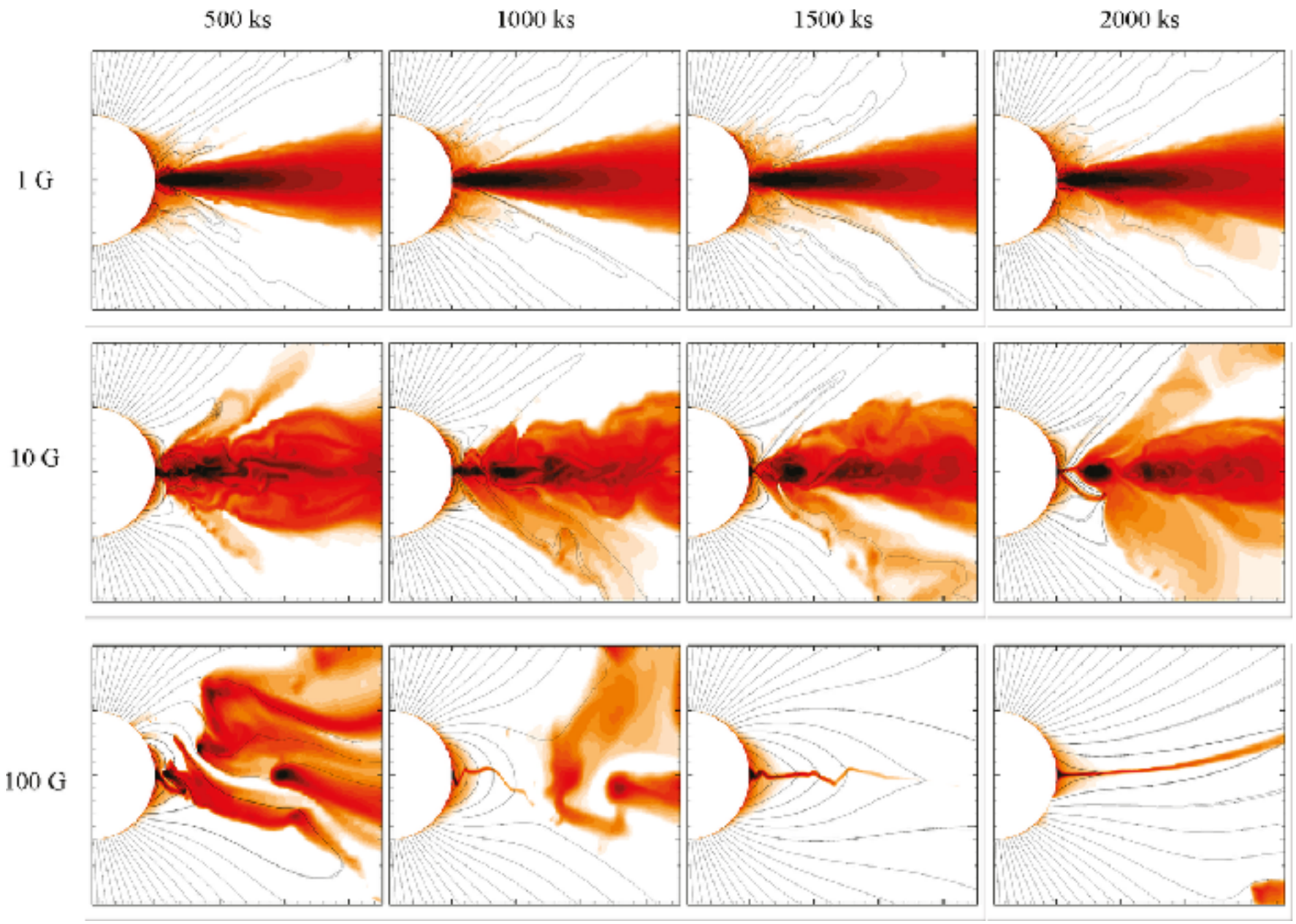

磁場が強いと円盤が壊れる (MHD simulation)

No. 52 V1094 Sco: a rare giant multi-ringed disk around a T Tauri star, S.E. van Terwisga et al. , A&Ap

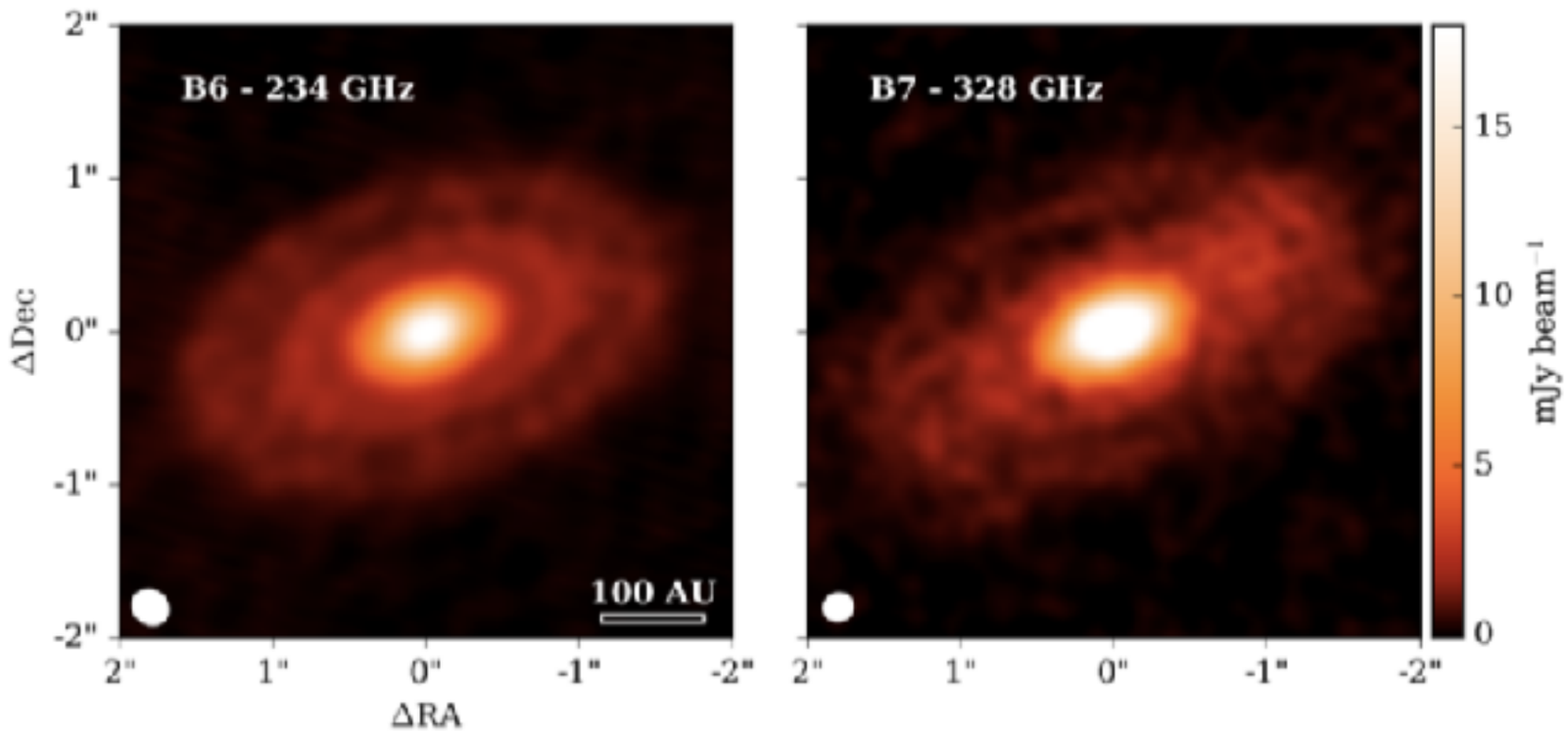

Lupus disk survey
(complete)

95 class II

R_{gas}/R_{dust} = 1.5-3

IM Lup, V1094
だけ例外的に
広がった円盤

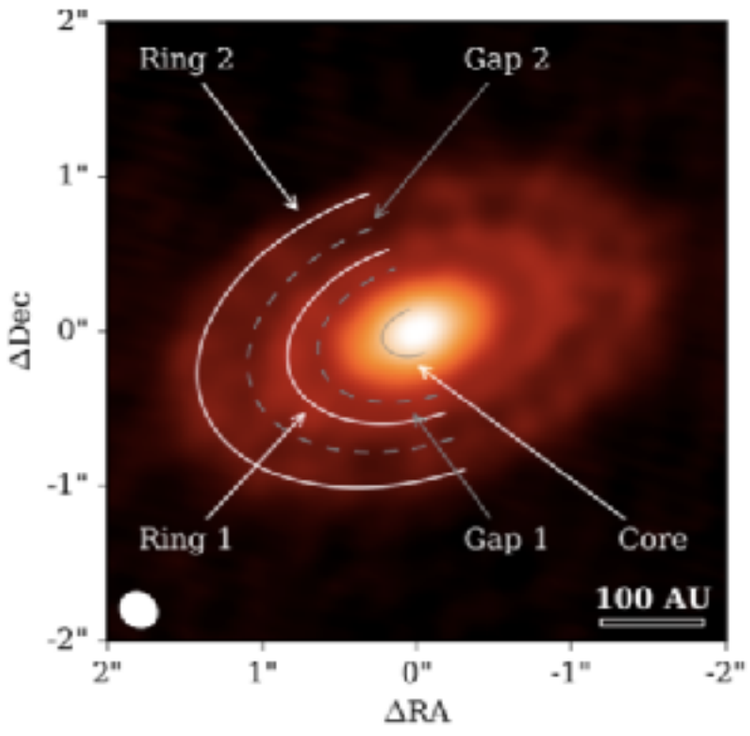

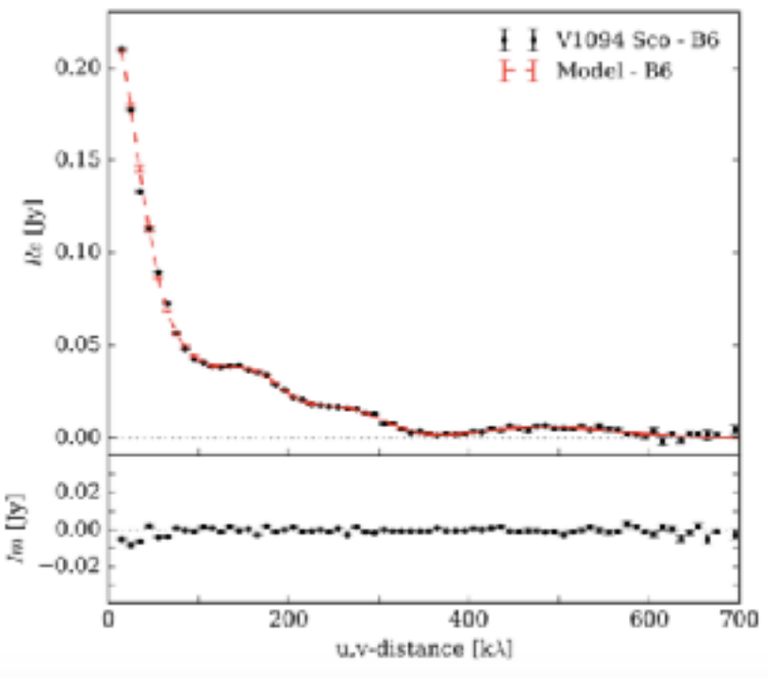

No. 53 VLTI/MIDI atlas of disks around low- and intermediate-mass young stellar object, J. Varga et al., A&Ap　(54頁，カタログ的)

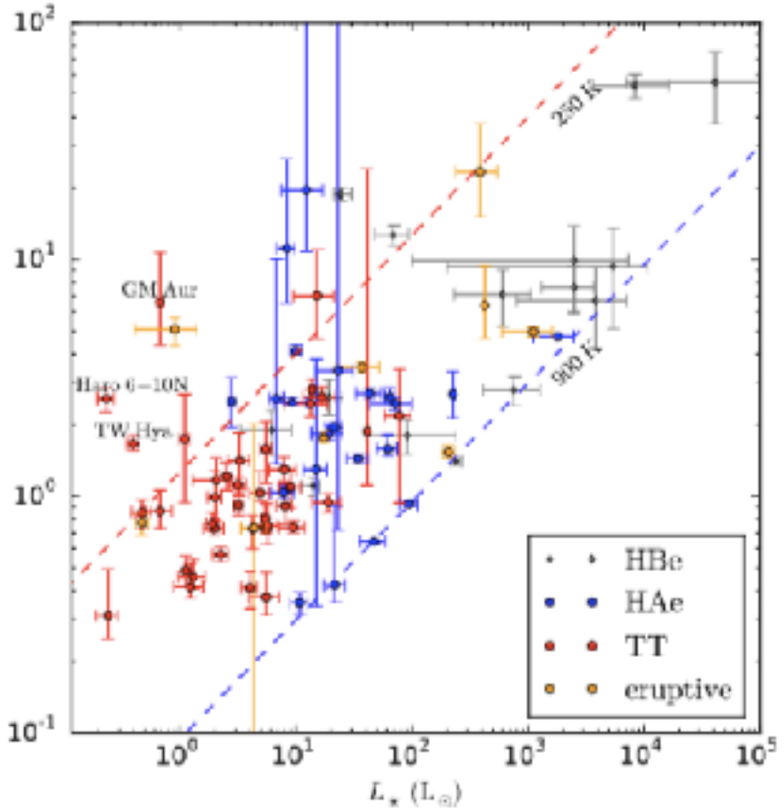

光度で規格化した円盤半径

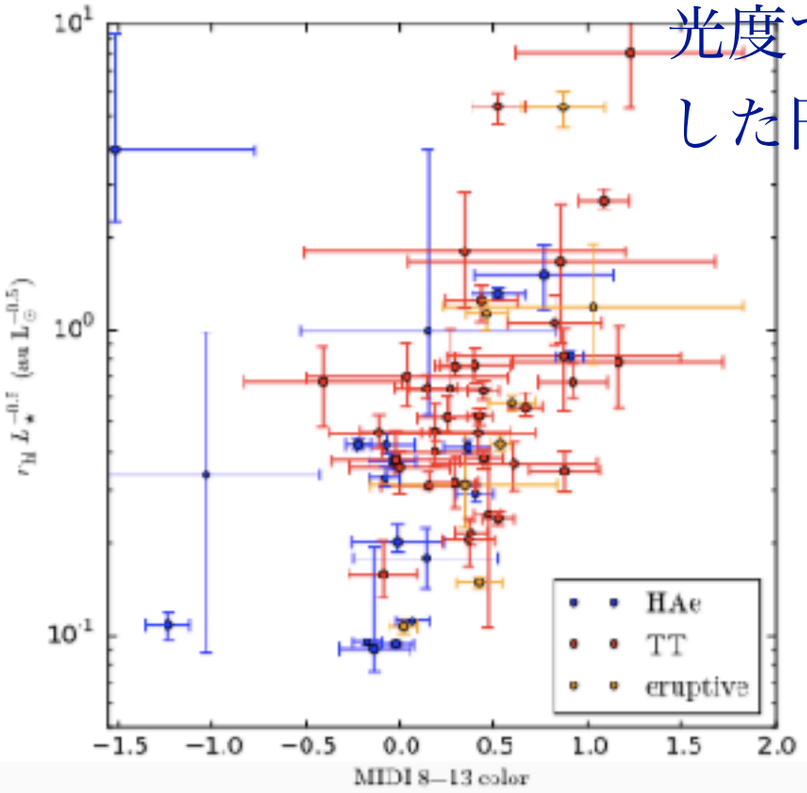

8μm-13μm 色

T Tau

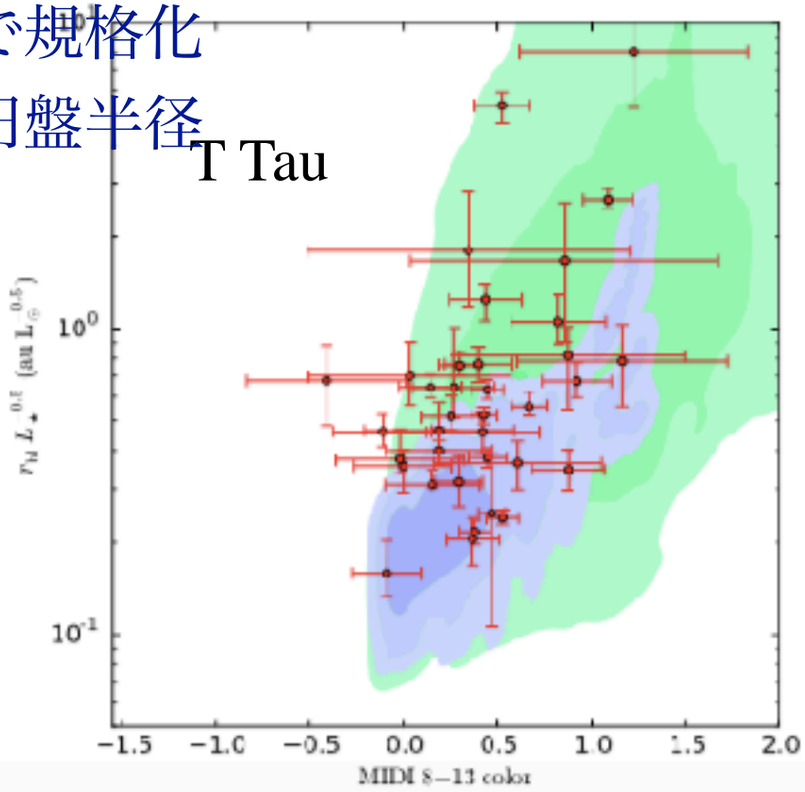

8μm-13μm 色

光度- MIRサイズ 関係:　T Tau 型星の方が HAe 型星より光度の割に低温で広がっている。

(AB Aur, HD 72106:　連星かも？　円盤に非対称性

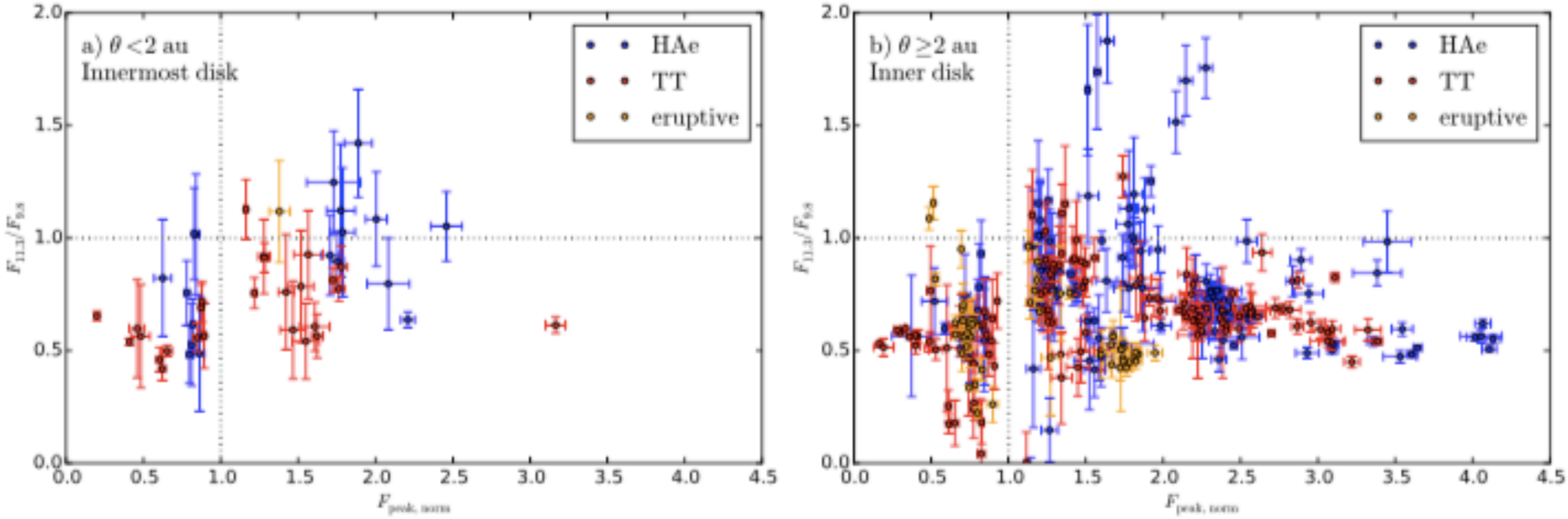

$r < 1$ au の最内縁は silicate feature が弱い

感度

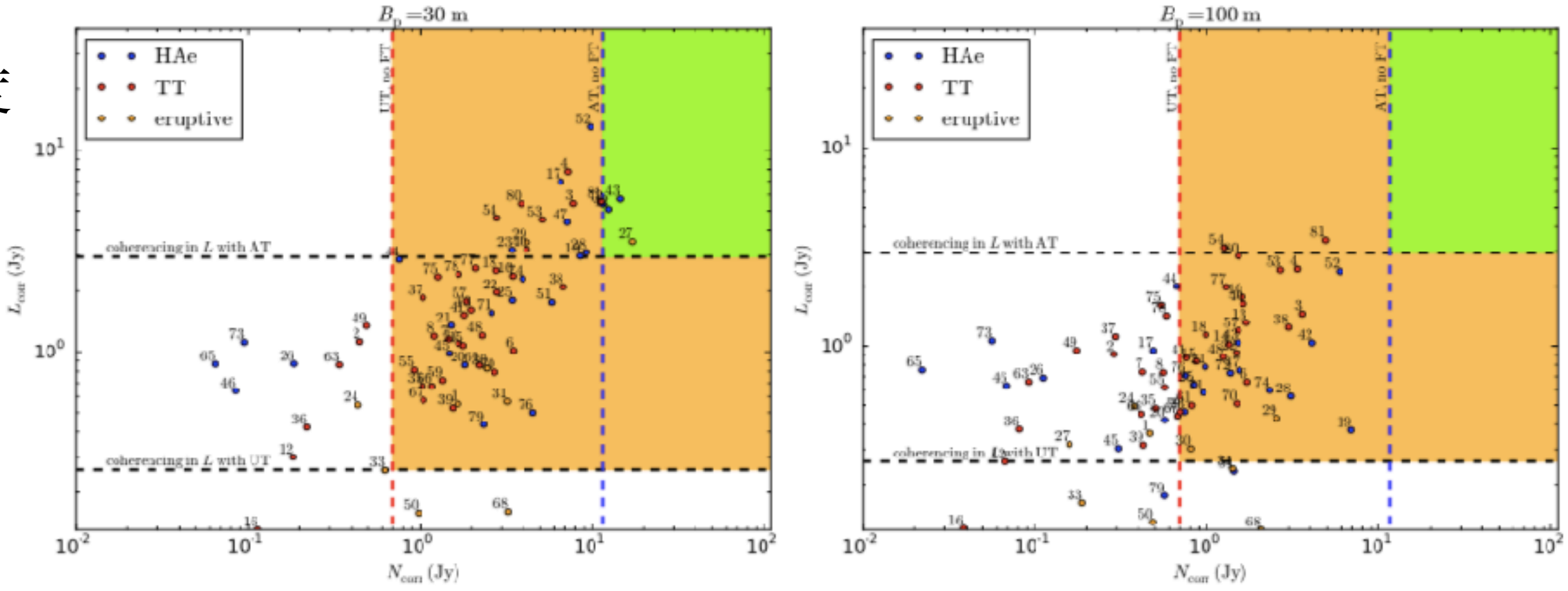

No. 54 Giant planets around FGK stars form probably through core accretion, Wei Wang et al. ApJ, 860, 136

Large Sky Area Multi-Object Fiber Spectroscopic Telescope (LAMOST)

によるPlanet-Metallicity (PM) relation の検証

偏り(バイアス)の除去

銀河内の金属量勾配

Teff, g で対照群を選択

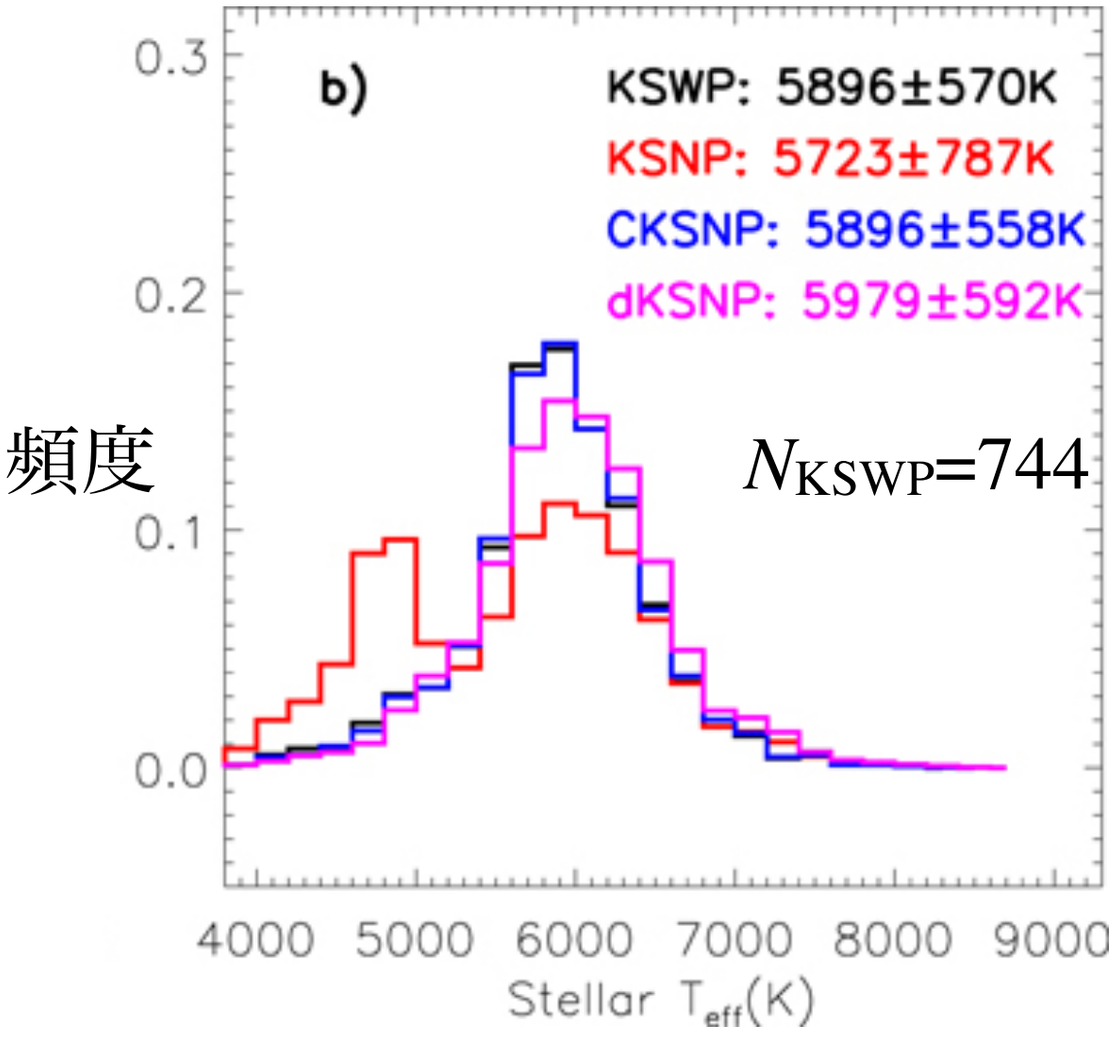

WP: 惑星あり NP: 惑星 検出なし

C=clean, d=dwarf

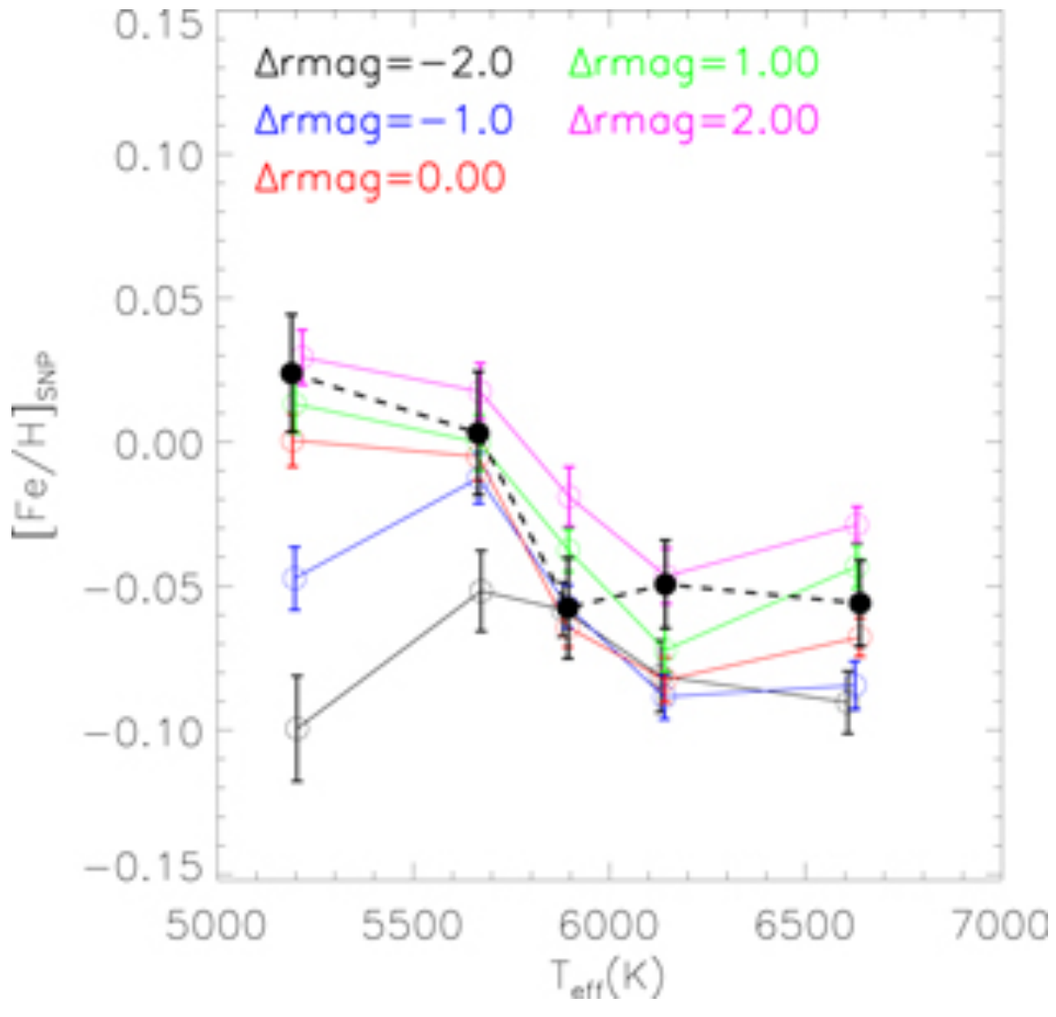

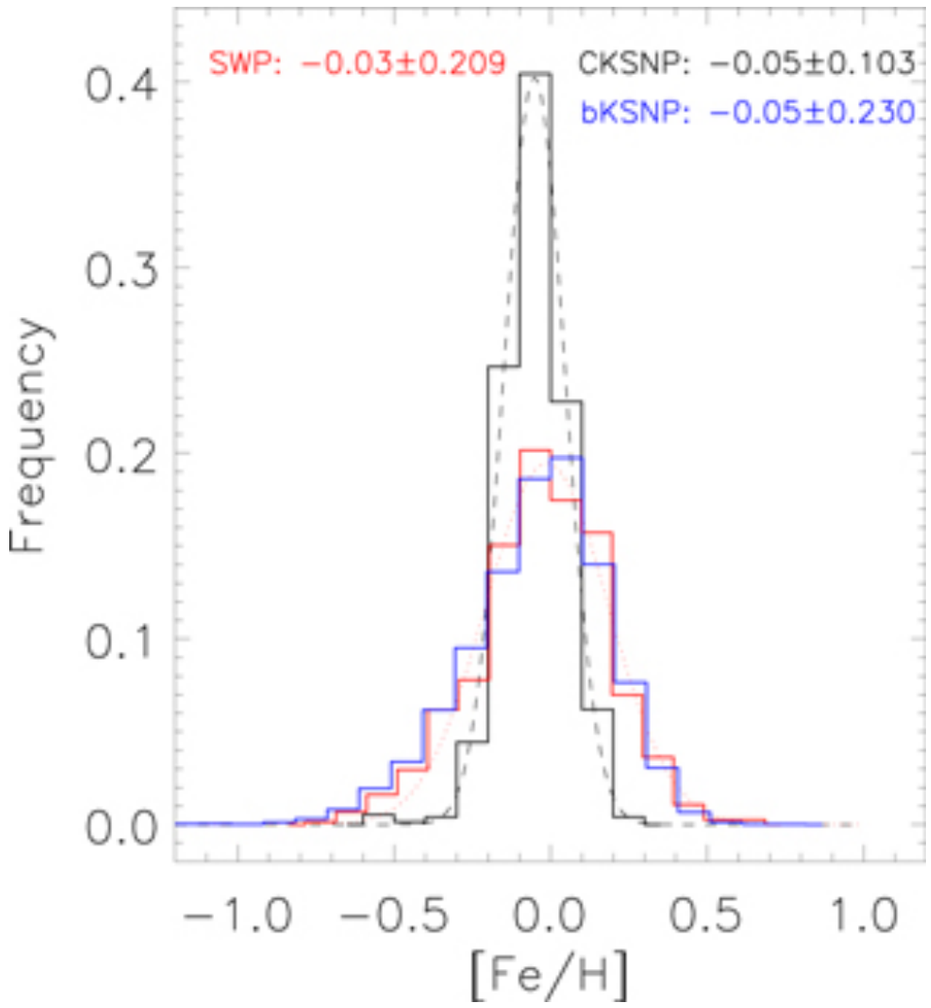

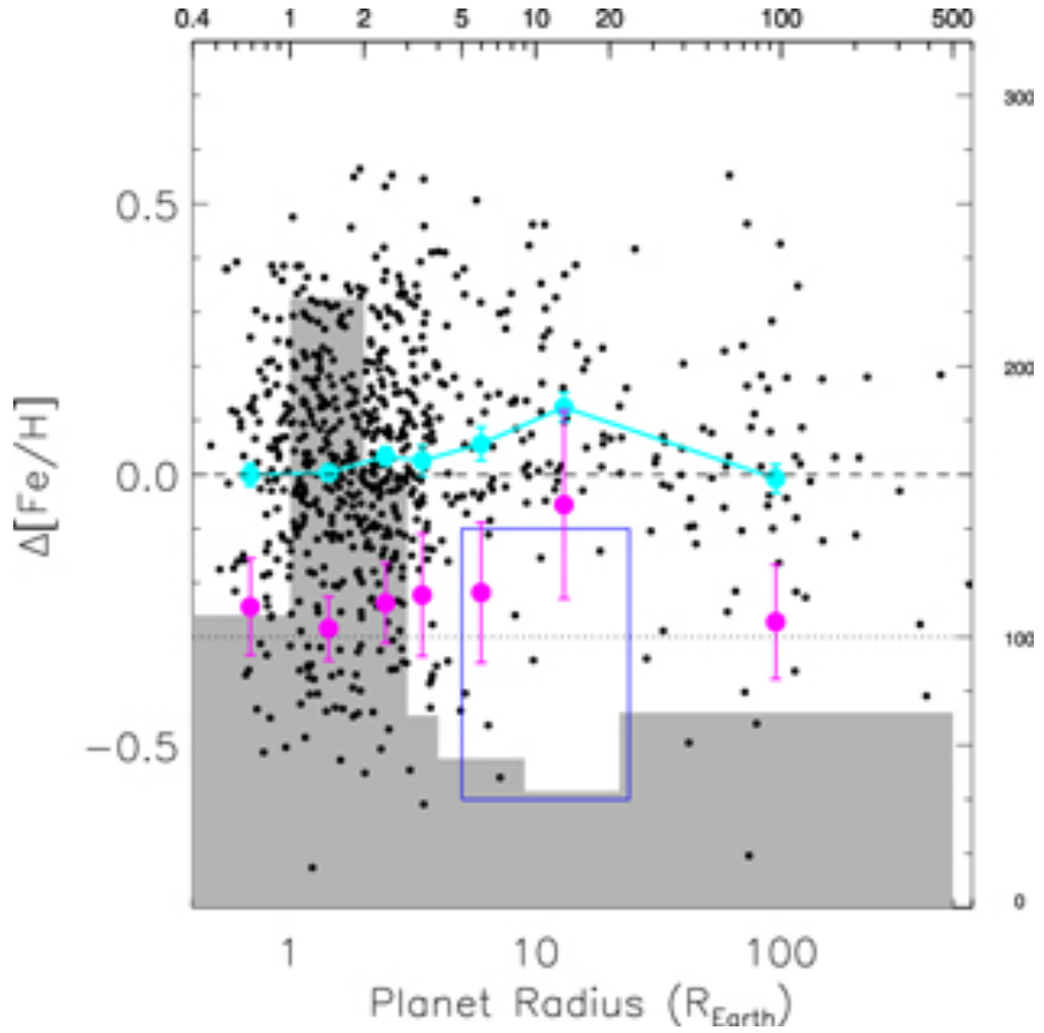

平均

統計揺らぎ

頻度

Δ[Fe/H] = ～0.00±0.03 dex (地球級), 0.06±0.03 (海王星級),

0.12±0.03 (木星級), -0.01±0.03 (さらに重い惑星or褐色矮星)

K型星では 2-4 R地球 で Δ[Fe/H] 0.1-0.2 dex

惑星落下による金属汚染説は正しくない。コア降着説を強く支持。